Electron-phonon resonance in InAs/GaSb type-II laser heterostructures

M. V. Kisin[a)]
Department of Electrical and Computer Engineering, SUNY at Stony Brook, Stony Brook, New York 11794

M. A. Stroscio[b)]
Electrical and Computer Engineering and Bioengineering Departments, University of Illinois at Chicago, Chicago, Illinois 60607

G. Belenky and S. Luryi
Department of Electrical and Computer Engineering, SUNY at Stony Brook, Stony Brook, New York 11794

(Received 1 October 2001; accepted for publication 22 January 2002)

The rate of interband electron transitions assisted by LO-phonon emission is studied in an InAs/GaSb double quantum well heterostructure, which models the active region of a type-II intersubband cascade laser. The main peak of the electron-phonon resonance corresponds to electron transitions from the lowest electron-like subband to the top of the highest light-hole-like subband that is displaced from the center of the Brillouin zone due to the asymmetry of the InAs/GaSb double quantum well heterostructure. © *2002 American Institute of Physics.* [DOI: 10.1063/1.1462873]

The process of the lower lasing state depopulation is essential for maintaining the population inversion in the active region of intersubband cascade lasers. For type-II ''broken-gap'' laser heterostructures, direct interband tunneling through the heterostructure ''leaky window'' δ has always been considered as a basic depopulation mechanism.[1–3] The rate of this process, Γ_{tun}, is determined by a small parameter $\varepsilon(\delta-\varepsilon)/E_{\text{GA}}E_{\text{GB}}$ [4], where ε is the kinetic energy of the tunneling electrons inside the window ($0<\varepsilon<\delta=150$ meV for InAs/GaSb interface) and $E_{\text{GA(B)}}$ are band gaps of the constituent semiconductors, InAs (A) and GaSb (B); see Fig. 1. The efficiency of the interband tunneling depopulation, therefore, decreases significantly when the depopulated level is located in the upper part of the leaky window, which would be the most favorable configuration from the standpoint of ensuring highest oscillator strength for the lasing transition and preventing thermal backfilling of the lower lasing state. In this letter, we demonstrate high efficiency of the interband depopulation assisted by LO-phonon emission, which has not yet been studied in type-II laser heterostructures. In type-I narrow gap heterostructures, the interband LO-phonon assisted tunneling has always been considered an inefficient process due to the symmetry difference between the conduction and valence band basis states.[5] However, in type-II heterostructures, band mixing and subband nonparabolicity effects inside the leaky window essentially remove this symmetry constraint. We also show that in coupled InAs and GaSb quantum wells (QWs) the anticrossing of the lowest electron-like and the highest light-hole-like levels provides for sufficiently strong overlap between electron and phonon states participating in the interband LO-phonon assisted transition, so that the rate of the process, Γ_{ph}, is quite comparable with the phonon-induced depopulation rate in type-I intersubband laser heterostructures.[6]

In this work, we consider LO-phonon assisted subband depopulation in an InAs/GaSb double quantum well (DQW) heterostructure, which models theactive region of a type-II intersubband laser, as depicted in Fig. 1. Initial and final electron states for the phonon emission process are described analytically in the framework of the six-band Kane model.[4] The width of the quasibound electron states inside the leaky window is determined by interband tunneling, $\Gamma\propto\Gamma_{\text{tun}}$, and in the upper part of the window is less than or about 1 meV.[4] This level broadening can be included in the Γ_{ph} rate calculations by using Lorentzian line shape function for the phonon emission transition. To optimize the depopulation of the lowest electron-like subband, LA1, we need to provide for anticrossing with the highest light-hole-like subband, LB1,

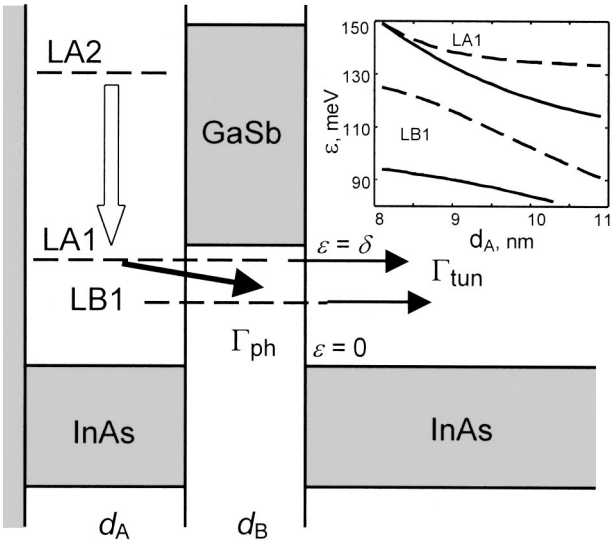

FIG. 1. Schematic band diagram of an active region of a type-II intersubband laser. The lasing transition is shown by block arrow. Solid arrows exemplify two main processes of the lower lasing state depopulation: direct interband tunneling through the heterostructure leaky window Γ_{tun}, and interband electron transition assisted by LO-phonon emission Γ_{ph}. Inset illustrates the anticrossing between two highest light-type energy levels in the leaky window. Electron in-plane momentum $K=0$. The width of the GaSb QW d_B is 6 nm (solid lines) and 10 nm (dashed lines).

a)Electronic mail: mvk@ece.sunysb.edu
b)Previously with U.S. Army Research Office, P.O. Box 12211, Research Triangle Park, NC 27709.

which also enhances the electron-phonon wave function overlap in the phonon emission process.[7] The inset in Fig. 1 shows the position of two highest light-type zone-centered energy levels in the heterostructure leaky window as a function of the InAs QW width d_A. The anticrossing condition roughly corresponds to the minimal separation between these levels and in our example occurs at $d_A \sim 9$ nm. Since the uppermost position of the LA1 subband reduces the thermal backfilling of the lower lasing states, it would be beneficial to keep LA1 as high as possible in the leaky window, still providing sufficient overlap with LB1 subband states. For this reason, we shall calculate and compare the LO-phonon emission rate for two different values of the InAs QW width, $d_A = 9$ nm and $d_A = 8.5$ nm, the latter allowing for the higher position of the subband LA1.

The upper limit for the phonon-assisted depopulation rate, Γ_{ph}, can be obtained assuming the final states for electron transitions to be unoccupied. Since the LO-phonon energies are very close in both constituent materials, $\hbar\omega_{\mathrm{LO}} \approx 30$ meV, we neglect polar mode confinement and calculate the phonon emission rate using 3D phonon approximation (3D PA),[8] that is assuming that the confined 2D electrons interact with dispersionless 3D bulk LO phonons. The effective electron-phonon coupling in 3DPA, $|M(q)|^2 = (\pi e^2 \omega_{\mathrm{LO}}/q)(1/\varepsilon_\infty - 1/\varepsilon_0)$,[8] after averaging with respect to the layer widths d_A and d_B, gives the rate of the spontaneous phonon emission in the form

$$\Gamma_{ph} = \frac{e^2\omega_{\mathrm{LO}}}{2}\left(\frac{1}{\varepsilon_\infty} - \frac{1}{\varepsilon_0}\right)\sum_f \int d^2\mathbf{q}\frac{I_{if}(q)}{q} \times \frac{\Gamma/2\pi}{[E_{\mathrm{LA1}}(0) - E_f(q) - \hbar\omega_{\mathrm{LO}}]^2 + (\Gamma/2)^2}, \quad (1)$$

$$I_{if}(q) = \int dz\,\psi_i^*(z)\psi_f(z)\int dz'\,\psi_f^*(z')\psi_i(z')e^{-q|z-z'|}. \quad (2)$$

For brevity, the initial electron state in the LA1 subband, ψ_i, is taken with zero in-plane momentum, so that the electron wave vector in the final state ψ_f is equal to the emitted phonon wave vector, $K_f = q$. With electron-phonon overlap $I_{if} = 1$, the last integral in Eq. (1) characterizes the effective density of the final states D_f in the subband E_f.

Figure 2 shows the depopulation rate Γ_{ph} calculated as a function of the GaSb QW width d_B for two different values of the InAs QW width. For a narrower InAs QW, the lower lasing subband LA1 has moved higher in the leaky window, and, as a result, all the resonances occur at larger values of the GaSb QW width, d_B. The increase of d_B in the range from 5 to 10 nm, while keeping the energy position of the initial electron-like subband LA1 practically unchanged, makes it possible to scan the final states in the hole-like subbands E_f, the light subband LB1 and the heavy subband H2, which thus move toward the upper part of the heterostructure leaky window. Figure 2 clearly demonstrates three distinctive regions in the LO-phonon emission rate, R1–R3, which are related to three consecutive resonances. The first, most remarkable resonance, R1, corresponds to the onset of the LA1→LB1 phonon-assisted transition, as illustrated in Fig. 3(a). The anticrossing between LA1 and LB1 subbands results in resonant penetration of the LA1 subband states into

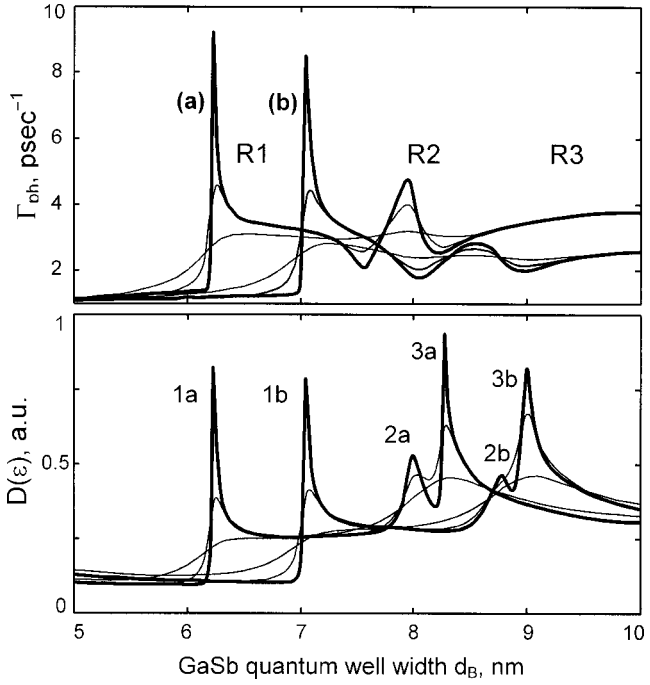

FIG. 2. Electron-phonon resonance in InAs/GaSb DQW heterostructure. Upper subplot shows LO-phonon emission rate Γ_{ph} calculated for two values of InAs QW width $d_A = 9$ nm (curve set a) and $d_A = 8.5$ nm (curve set b). Smaller width of the InAs QW provides for the higher position of the lower lasing states in the leaky window. Three regions of the phonon emission rate, R1–R3, correspond to three different type of resonant transition in Brillouin zone. Lower subplot shows the total effective density of the final electron states $D(\varepsilon)$ for the phonon emission transitions. Level broadening Γ is taken 0.1 meV (thick solid lines), 1 meV, and 5 meV (thin lines in each curve set).

the adjacent GaSb QW B and ensures sufficient electron-phonon overlap for this indirect interwell A→B transition. R1-related transitions are also indirect in the K space, since the top of the upper light-hole-like subband LB1 is displaced to the final value of K due to the subband spin splitting inherent to asymmetric DQW heterostructures.[9] This splitting is especially strong in type-II heterostructures based on the narrow-gap InAs/GaSb material system. In Figure 3(a), for convenience, we show the split subbands with only one sign of the spin polarization. The Kramers degeneracy condition $E_\uparrow(K) = E_\downarrow(K)$, imposed on any system by time-reversal symmetry, should be used here to restore the complete subband structure. Note, that the final momentum transfer is important for the high phonon emission rate in R1 resonance, because the optimum value of the electron-phonon overlap $I(q)$ can be engineered close to the peak of the effective density of the final electron states at the top of the LB1 subband [see Fig. 3(b) and corresponding peaks 1(a) and 1(b) in the lower subplot of Fig. 2].

With d_B increasing, phonon-assisted LA1→LB1 transitions become less efficient, first, because of corresponding decrease of the effective final density of states away from the top of the LB1 subband, and second, due to the suppression of the electron-phonon overlap $I(q)$ both at the small and large momentum transfers. This can be readily seen in Fig. 4, showing the electron-phonon overlap integrals for interband transitions as a function of the transferred (phonon) wave vector $q = K_f$. For a "vertical" transition with zero momentum transfer ($q = 0$), the electron-phonon overlap integral

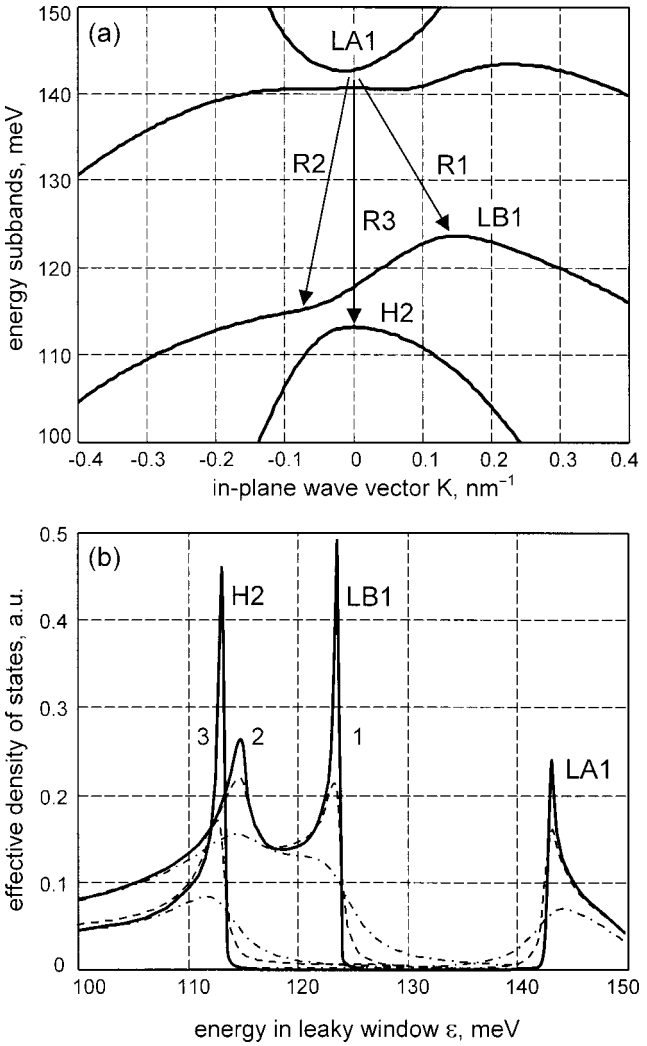

FIG. 3. Energy spectrum of an InAs/GaSb DQW with layer widths $d_A = 8.5$ and $d_B = 9$ nm. (a) Band diagram of the electron energy subbands in the upper part of the leaky window illustrating three basic interband transitions assisted by the LO-phonon emission. The most important resonant transition, R1, is indirect in Brillouin zone. (b) Effective density of states for electron subbands participating in the phonon–emission transitions. Level broadening parameter is $\Gamma = 0.1$ meV (solid lines), 1 meV (dashed lines), and 5 meV (dashed–dotted lines).

$I(q)$ is reduced to the overlap between orthogonal initial and final electron states, and thus vanishes. This explains the pronounced minimum in the phonon emission rate between the peaks R1 and R2. The final electron states for the latter resonance belong to the ring of the LB1 subband saddle points, which are again characterized by a high efficient density of states; see Fig. 3(b) and peaks 2a and 2b in the lower subplot of Fig. 2. For $d_A = 9$ nm, the peak of the effective density of states is more pronounced and is also favorably located at small negative values of K_f, where the electron-phonon overlap for LA1(0)→LB1(K) electron transition is again significant (see Fig. 4). For $d_A = 8.5$ nm, both the density peak 2b and electron-phonon overlap are smaller and, correspondingly, thepeak rate value R2 is relatively small. Finally, the increase of the phonon emission rate in the region R3 corresponds to the onset of electron transitions into the H2 subband. The overall rate of the phonon emission is significantly depressed because the most important transitions to the subband top, characterized by the highest effective density of states (peaks P3a and P3b in the lower subplot of Fig. 2) correspond to inefficient vertical transitions with nearly zero electron/heavy-hole overlap integral $I(q)$. Most of the R3 rate is actually determined by the transitions to the H2-subband states with $K_f < -0.1\ \mathrm{nm}^{-1}$, where the LA1-H2 overlap significantly increases due to the light-heavy state mixing effect in the H2 subband (see Fig. 4).

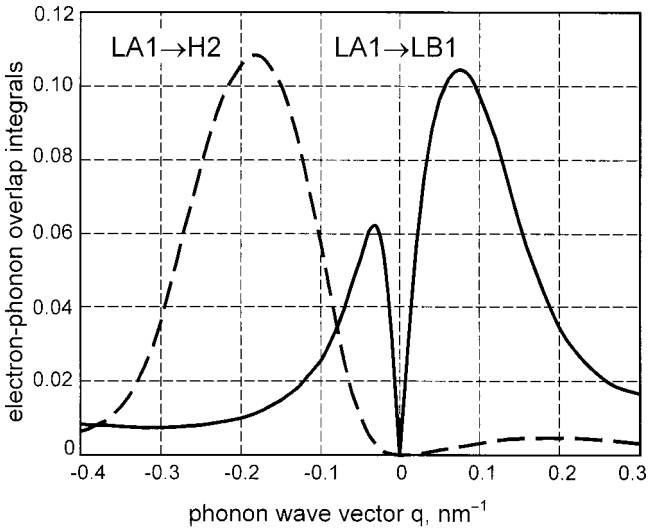

FIG. 4. Electron-phonon overlap integral $I(q)$ for LA1→LB1 (solid line) and LA1→H2 (dashed line) transitions in an InAs/GaSb DQW with layer widths $d_A = 9$ nm and $d_B = 8$ nm.

In conclusion, we compare the LO-phonon emission rates calculated for two different values of the InAs QW width; see the upper plot in Fig. 2. For a narrower InAs QW, represented by curve set (b), the lower lasing subband LA1 has been relocated to the extreme upper end of the leaky window. Still, the overall magnitude of the main peak R1 remains practically unchanged. This means that phonon-assisted depopulation can be conveniently employed even when the lower lasing level is designed near the upper edge of the heterostructure leaky window, where direct interband tunneling depopulation becomes inefficient.

This work was supported by U.S. Army Research Office and Grant No. DAAD 190010423.

[1] R. Q. Yang and J. M. Xu, Appl. Phys. Lett. **59**, 181 (1991).
[2] H. Ohno, L. Esaki, and E. E. Mendez, Appl. Phys. Lett. **60**, 3153 (1992).
[3] J. R. Meyer, C. A. Hoffman, and F. J. Bartoli, Appl. Phys. Lett. **67**, 757 (1995).
[4] M. V. Kisin, M. A. Stroscio, S. Luryi, and G. Belenky, Physica E (Amsterdam) **10**, 576 (2001).
[5] Yu. B. Lyanda-Geller and J.-P. Leburton, Appl. Phys. Lett. **67**, 1423 (1995).
[6] J. Faist, F. Capasso, C. Sirtori, D. L. Sivco, A. L. Hutchinson, M. S. Hybertsen, and A. Y. Cho, Phys. Rev. Lett. **76**, 411 (1996).
[7] M. A. Stroscio, M. V. Kisin, G. Belenky, and S. Luryi, Appl. Phys. Lett. **75**, 3258 (1999).
[8] J. K. Jain and S. Das Sarma, Phys. Rev. Lett. **62**, 2305 (1989); S. Das Sarma, V. B. Campos, M. A. Stroscio, and K. W. Kim, Semicond. Sci. Technol. **7**, B60 (1992); for a general discussion of phonon processes in nanostructures see M. A. Stroscio and M. Dutta, *Phonons in Nanostructures* (Cambridge University Press, Cambridge, 2001).
[9] G. Goldoni and A. Fasolino, Phys. Rev. Lett. **69**, 2567 (1992).